

Electron Transfer at Molecule–Metal Interfaces under Floquet Engineering: Rate Constant and Floquet Marcus Theory

Yu Wang and Wenjie Dou*

Cite This: *ACS Phys. Chem Au* 2024, 4, 160–166

Read Online

ACCESS |

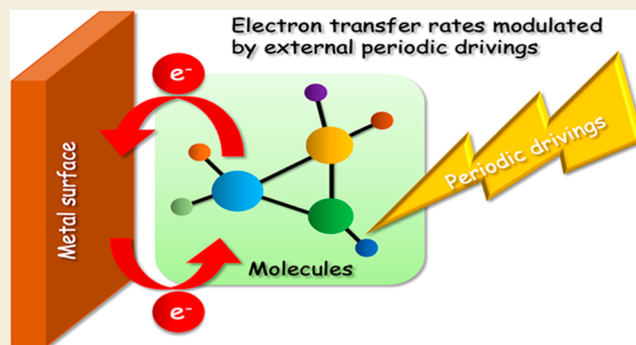
Metrics & More

Article Recommendations

Supporting Information

ABSTRACT: Electron transfer (ET) at molecule–metal or molecule–semiconductor interfaces is a fundamental reaction that underlies all electrochemical processes and substrate-mediated surface photochemistry. In this study, we show that ET rates near a metal surface can be significantly manipulated by periodic driving (e.g., Floquet engineering). We employ the Floquet surface hopping and Floquet electronic friction algorithms developed previously to calculate the ET rates near the metal surface as a function of driving amplitudes and driving frequencies. We find that ET rates have a turnover effect when the driving frequencies increase. A Floquet Marcus theory is further formulated to analyze such a turnover effect. We then benchmark the Floquet Marcus theory against Floquet surface hopping and Floquet electronic friction methods, indicating that the Floquet Marcus theory works in the strong nonadiabatic regimes but fails in the weak nonadiabatic regimes. We hope these theoretical tools will be useful to study ET rates in the plasmonic cavity and plasmon-assisted photocatalysis.

KEYWORDS: electron transfer rate, Floquet engineering, molecule–metal interface, nonadiabatic dynamics, Marcus theory



INTRODUCTION

Electron transfer (ET) at molecule–metal or molecule–semiconductor interfaces is of interest to many research fields,¹ including surface photochemistry,² surface catalysis,³ chemisorption,⁴ and dye-sensitized solar cells (DSSCs).⁵ Depending on whether one changes the chemical structure of the interfaces, there exist chemical and physical means to manipulate the ET processes. Using acceptor units with strong electron-withdrawing capability within dye molecules for DSSCs⁶ or constructing heterostructures to form a heterojunction in photocatalysis⁷ falls into the first category. Floquet engineering, on the other hand, serves as a physical means to modulate ET rates without chemical structure modifications.⁸

Floquet engineering is a term that refers to using external periodic driving to control quantum systems.^{9–11} When subjected to external periodic driving, the physical properties of the system can change dramatically. Notably, the hybrid state from the system and the external driving form a type of quantum matter, such that Floquet engineering is a popular tool to achieve new phases of quantum matter, such as Floquet topological insulators,¹² Floquet time crystals,¹³ and Floquet superconductors.¹⁴ In reality, periodic driving can be achieved by, for example, surface plasmon, which is the collective oscillations of free electrons in the metal.¹⁵ Light, as an electromagnetic field, can also serve as a tool to achieve Floquet engineering. Under such Floquet engineering, the

transport of energy and charge in organic semiconductors can be enhanced. For example, the electrical conductivities of different n-type organic semiconductors were enhanced when deposited on top of a plasmonic resonator.¹⁶ When a p-type semiconductor was ultrastrongly coupled to plasmonic modes, both the conductivity and photoconductivity were enhanced.¹⁷ In a properly designed, strongly coupled system in the cavity, experiments showed efficient energy transfer beyond the Förster limit in spatially separated entangled molecules.¹⁸ To the best of our knowledge, there is little theoretical investigation on how ET rates are modified by light or periodic drivings. Therefore, in this study, we provide a theoretical formulation of ET rates under periodic driving conditions, particularly at molecule–metal interfaces.

To solve the time-periodic problem, we can employ Floquet theory. Floquet theory is used to map the time-periodic drivings into a time-independent hybrid quantum state, which accounts for a variety of new phenomena in many quantum systems, including laser-driven atoms,¹⁹ strongly correlated

Received: September 10, 2023

Revised: December 5, 2023

Accepted: December 5, 2023

Published: December 21, 2023



electron systems,^{20,21} electron–phonon systems,^{22,23} and quantum transport.^{24–27} For simpler model systems, there exist methods based on the Floquet theory, including the Floquet Green function,^{28–30} the Floquet dynamical mean-field theory (DMFT),^{31,32} and the Floquet scattering theory.^{33–35} For more realistic systems, the Floquet surface hopping (FSH) approach serves as a tool to deal with nonadiabatic molecular dynamics in the gas phase or in solution under the influence of Floquet engineering.^{36,37}

Recently, we developed an alternative Floquet surface hopping method to deal with nonadiabatic molecular dynamics at molecule–metal interfaces.³⁸ The Floquet surface hopping method is based on the Floquet classical master equation (FCME). Furthermore, when the hybrid electron–light states move faster than the nuclear motion (weak nonadiabatic regimes), we can map the FCME into a Floquet–Fokker–Planck (FFP) equation. This mapping greatly simplifies the nonadiabatic dynamics with Floquet drivings, such that one can solve the typical Langevin dynamics with explicit friction and random force from the hybrid electron–light states.³⁹

In this study, we apply our FSH method to study the ET rates at the molecule–metal interface under the influence of Floquet drivings. The model we applied here can be viewed as an extension of the Floquet-driven spin-boson model with one donor coupled to a continuum of acceptors. In the limit of a strong nonadiabatic regime (small molecule–metal couplings Γ), we formulate the Floquet version of the Marcus theory, which agrees with FSH results very well. In the limit of the weak nonadiabatic regime, FEF agrees well with FSH results. In both limits, we find that ET rates increase monotonically as a function of driving amplitudes, whereas there is a turnover effect of ET rates as a function of driving frequencies; namely, the ET rates first increase and then decrease with the driving frequency. Such a turnover effect is further confirmed by our analysis of the gradient of the ET rate with the respective driving frequency. To apply our Floquet Marcus theory for realistic systems, one of the experimental situations is the plasmon-enhanced catalysis, where one uses light to create plasmonic excitation that assists ET rate at molecule–metal interfaces.⁴⁰ A similar realistic situation is the plasmonic cavity, where the light and matter can be strongly coupled within a cavity.⁴¹ The Floquet Marcus theory can be used to study the ET rate inside a plasmonic cavity. We conclude that although the Floquet drivings increase the overall ET rate, there is an optimal driving frequency that maximizes the ET rate. ET rates are widely concerned in the field of electrochemistry or plasmonic cavity; therefore, we believe our theoretical prediction of ET rate modulations by external periodic drivings at the molecule–metal interface could provide a guidance to experiments.

METHODS

We consider ET at the molecule–metal interface, where one molecular energy level couples to nuclear DOFs and a continuum of electronic states from the metal surface. The total Hamiltonian of the whole system is given by

$$\hat{H} = \hat{H}_S + \hat{H}_B + \hat{H}_T \quad (1)$$

$$\hat{H}_S = (E(x) + A \sin(\Omega t)) d^\dagger d + V_0(x) + \frac{p^2}{2m} \quad (2)$$

$$\hat{H}_B = \sum_k \varepsilon_k c_k^\dagger c_k \quad (3)$$

$$\hat{H}_T = \sum_k V_k (d^\dagger c_k + c_k^\dagger d) \quad (4)$$

Here, we divide the total Hamiltonian into three parts: the molecule \hat{H}_S , the metal \hat{H}_B , and the interactions between them \hat{H}_T . $d(d^\dagger)$ and $c_k(c_k^\dagger)$ are the annihilation (creation) operators for an electron at the molecular energy level (subsystem) and at the metal surface (electronic bath). ε_k is the energy level of electrons in the metal. V_k is the coupling strength between the electronic level in the metal and that in the molecule. $E(x)$ is the on-site energy of the molecular level, which can be an arbitrary function of the nuclear position. $V_0(x)$ is the diabatic potential energy surface (PES) of the unoccupied state. We can further define the diabatic PES for the time-independent occupied state as $V_1(x) = V_0(x) + E(x)$. Without loss of generality, we assume that the diabatic potential V_0 is the parabolic

$$V_0(x) = \frac{1}{2} m \omega^2 x^2 \quad (5)$$

Here, ω is the frequency of the nuclear motion and m is the mass of the oscillator. Furthermore, we define $E(x) = gx\sqrt{2m\omega/\hbar} + E_d$, where g represents electron–phonon (el–ph) coupling strength and E_d is the energy of the occupied molecular level without Floquet drivings, such that the occupied PES $V_1(x) = V_0(x) + E(x)$ is the shifted harmonic oscillator.

The periodic driving acting on the molecular energy level has a driving amplitude A and a driving frequency Ω in this model. This external driving can be viewed as light coupling to the dipole of the molecule near the metal surface. The key parameters for this model are the nuclear frequency (ω), the temperature of the metal surface (T), the el–ph coupling strength (g), and the molecule–metal interaction [$\Gamma(\varepsilon) = 2\pi \sum_k |V_k|^2 \delta(\varepsilon_k - \varepsilon)$]. Γ is assumed to be a constant under the wide band approximation.

We also restrict ourselves in the high-temperature regime ($kT \gg \hbar\omega, \Gamma$), such that we can employ the Floquet surface hopping dynamics to treat the nuclear motion classically. The Floquet surface hopping algorithm is proposed in ref 38 to calculate the nonadiabatic dynamics of the electron population under the influence of different Floquet drivings. We then extract the ET rate by exponential fitting for the electron population.⁴² To be more explicit, in FSH dynamics, we use the phase space densities $P_0(x, p, t)$ and $P_1(x, p, t)$ to represent the probability density for the electronic molecular level to be unoccupied (occupied) at time t with the nucleus at position (x, p) . The equations of motion for the probability densities are given by the FCMEs

$$\begin{aligned} \frac{\partial P_0(x, p, t)}{\partial t} &= \frac{\partial V_0(x, p)}{\partial x} \frac{\partial P_0(x, p, t)}{\partial p} - \frac{p}{m} \frac{\partial P_0(x, p, t)}{\partial x} \\ &\quad - \frac{\Gamma}{\hbar} \mathfrak{R}(\tilde{f}(E(x), t)) P_0(x, p, t) \\ &\quad + \frac{\Gamma}{\hbar} (1 - \mathfrak{R}(\tilde{f}(E(x), t))) P_1(x, p, t) \tilde{f}(E(x), t)) \\ &\quad P_1(x, p, t) \end{aligned} \quad (6)$$

$$\begin{aligned} \frac{\partial P_1(x, p, t)}{\partial t} &= \frac{\partial V_1(x, p)}{\partial x} \frac{\partial P_1(x, p, t)}{\partial p} - \frac{p}{m} \frac{\partial P_1(x, p, t)}{\partial x} \\ &\quad + \frac{\Gamma}{\hbar} \mathfrak{R}(\tilde{f}(E(x), t)) P_0(x, p, t) \\ &\quad - \frac{\Gamma}{\hbar} (1 - \mathfrak{R}(\tilde{f}(E(x), t))) P_1(x, p, t) \tilde{f}(E(x), t)) \\ &\quad P_1(x, p, t) \end{aligned} \quad (7)$$

Note that the FCME is derived under the condition that the bandwidth is much larger than the frequency of the periodic field. The Floquet CME and Floquet Marcus rates can both apply to the case when the electronic state energy gap is larger than the oscillator

frequency of the periodic field. Here, $\tilde{f}(E(x), t)$ is a Bessel function modified by the Fermi function

$$\tilde{f}(E(x), t) = \left(\sum_{p,q} (i)^p (-i)^q J_p(z) J_q(z) e^{i(p-q)\Omega t} f(E(x) - q\Omega) \right) \quad (8)$$

and $f(E(x) - q\Omega) = 1/(1 + e^{\beta(E(x) - q\Omega)})$ is the Fermi function ($\beta \equiv 1/kT$). J_p is the Bessel function. p is an integer ranging from $-\infty$ to $+\infty$. In calculation, we need to truncate the value of p according to $\frac{A}{\Omega}$, see details in ref 38. Note that the above equation of motion is derived from the real-time response to periodic external potentials.³⁸ For the model we used here, the Floquet theorem yields the same equation of motion as the real-time response to periodic external potential after we trace the Floquet replica. Please see ref 43 for a proof of the equivalence of the two approaches. Note that only the real part of $\tilde{f}(E(x), t)$ appears in FCME. When taking the cycle average, eq 8 becomes

$$\bar{\tilde{f}}(E(x), t) = \int_0^T \tilde{f}(E(x), t) dt = \sum_p J_p(z)^2 f(E(x) - p\Omega) \quad (9)$$

In ref 38, we have proposed two different trajectory-based surface hopping algorithms to solve the FCME. The first one is denoted as FaSH, where we propagate the trajectories on one of the two diabatic potentials V_0 and V_1 with stochastic hopping between them. The hopping rates are the cycle-averaged ones

$$\gamma_{0 \rightarrow 1} = \frac{\Gamma}{\hbar} \bar{\tilde{f}}(E(x)) \quad (10)$$

$$\gamma_{1 \rightarrow 0} = \frac{\Gamma}{\hbar} (1 - \bar{\tilde{f}}(E(x))) \quad (11)$$

In FaSH, the electron populations are cycle-averaged ones. To reproduce the oscillations within the cycle, we also introduced the FaSH-density algorithm. In addition to the FaSH algorithm, for each trajectory, we also propagate the electron densities

$$\frac{\partial \sigma_0(t)}{\partial t} = -\frac{\Gamma}{\hbar} \Re(\tilde{f}(E(x), t)) \sigma_0(t) + \frac{\Gamma}{\hbar} (1 - \Re(\tilde{f}(E(x), t))) \sigma_1(t) \quad (12)$$

$$\frac{\partial \sigma_1(t)}{\partial t} = \frac{\Gamma}{\hbar} \Re(\tilde{f}(E(x), t)) \sigma_0(t) - \frac{\Gamma}{\hbar} (1 - \Re(\tilde{f}(E(x), t))) \sigma_1(t) \quad (13)$$

We use the electron densities to calculate the electron population. Note that we use the noncycle-averaged \tilde{f} in the above equations, such that the oscillations within the cycle are recovered in the FaSH-density algorithm. See ref 38 for more details.

In the limit of small Γ , the ET rate can be determined analytically by Marcus theory.⁴⁴

$$k_{0 \rightarrow 1} = \int_{-\infty}^{+\infty} d\varepsilon \Gamma \bar{\tilde{f}}(\varepsilon) \frac{e^{-(E_r - \varepsilon + \bar{E}_d)^2 / 4E_r kT}}{\sqrt{4\pi E_r kT}} \quad (14)$$

$$k_{1 \rightarrow 0} = \int_{-\infty}^{+\infty} d\varepsilon \Gamma (1 - \bar{\tilde{f}}(\varepsilon)) \frac{e^{-(E_r + \varepsilon + \bar{E}_d)^2 / 4E_r kT}}{\sqrt{4\pi E_r kT}} \quad (15)$$

where $E_r = g^2/\hbar\omega$ is the reorganization energy. Note that in the Marcus picture, the horizontal shift of two parabolas (Q) is defined as the electron–phonon coupling strength (g). Note also that the horizontal shift and the frequency of the parabolas determine the reorganization energy ($E_r = \hbar\omega Q^2$). $\bar{E}_d = E_d - E_r$ is the renormalized electron energy. Note that, in the limit of small Γ without Floquet driving, we have proven that the surface hopping ET rate agrees with the Marcus theory.⁴⁴ With Floquet driving, the Fermi function $f(\varepsilon)$ in the Marcus theory is replaced by the cycle-averaged one, $\bar{\tilde{f}}(\varepsilon)$, such

that the Floquet Marcus theory should agree with the results from FaSH. This is indeed the case (see Results section for discussion). Note that the Marcus rate has been applied in realistic systems for ET at molecule–metal and molecule–semiconductor interfaces.^{45,46} Knowing the strength of the light–matter interactions, the Floquet Marcus theory can be applied to realistic systems to study ET rates at molecule–metal and molecule–semiconductor levels as well. The strength of the light–matter interactions may be calculated ab initio.⁴⁷

In the limit of slow nuclear motion ($\Gamma > \hbar\omega$), the FCME can be mapped onto a Fokker–Planck equation. The Fokker–Planck equation is then solved by Floquet electronic friction (FEF) Langevin dynamics.³⁹ The FEF method will also be used to study the ET rate. See Appendix A in Supporting Information for a detailed discussion.

RESULTS

We first plot ET rates as a function of nuclear friction γ_n under Floquet driving in Figure 1. The nuclear friction can be seen as

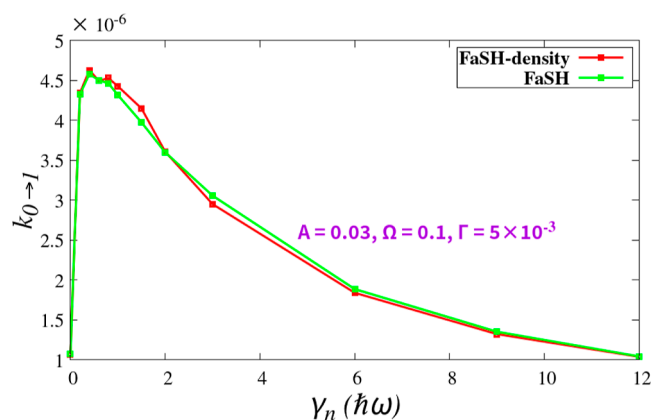


Figure 1. ET rates near the metal surface as a function of nuclear friction γ_n under a Floquet driving ($A = 0.03$, $\Omega = 0.1$) at a large Γ limit. $kT = 0.01$, $\omega = 0.003$, $g = 0.025$, and $E_d = \frac{g^2}{\hbar\omega}$.

the frictional effects from the solvent or surface nuclear motion. We used atomic units in our calculations. Notice that there is optimal nuclear friction that predicts maximal ET rates. This is exactly the Kramer turnover effect. Such a trend is very similar to the case in the ET process near metal surfaces without any Floquet driving, see ref 48. Below, we will mainly study the regime where the ET rates do not strongly depend on γ_n , namely, $\gamma_n = \hbar\omega$.

In Figure 2, we plot the ET rate from the metal to the molecule $k_{0 \rightarrow 1}$ from Floquet Marcus theory, FaSH-density, and FaSH and FEF methods. Note that the results from the FaSH-density and FaSH methods are almost identical. In the limit of small Γ , the Marcus rate agrees with FaSH-density (and FaSH) very well. This is the strong nonadiabatic limit. As seen from eq 14, the Floquet Marcus theory predicts that the ET depends linearly on Γ . In the weak nonadiabatic limit when Γ is large enough, FaSH-density (and FaSH) predicts a plateau for the rates as a function of Γ . This is also captured by the FEF method. However, the Marcus rate fails in this weak nonadiabatic regime. When we further increase Γ , we expect that the rates will grow exponentially with Γ due to the broadening effects. Notice that the broadening effects are not included here. Our methods fail in the very large Γ limit. Such a trend is very similar to the case without Floquet driving.⁴⁹ Note also that without Floquet driving, we have shown that the electronic friction method can predict the correct rates when Γ

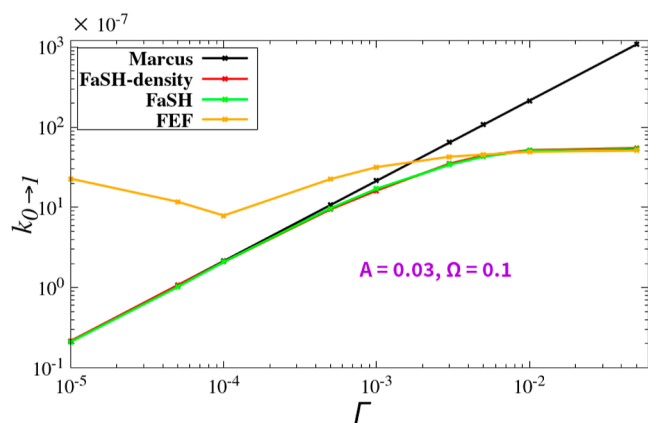


Figure 2. ET rates near the metal surface as a function of Γ for four algorithms. $kT = 0.01$, $\omega = 0.003$, $g = 0.025$, $E_d = \frac{g^2}{\hbar\omega}$, $A = 0.03$, $\Omega = 0.1$, and nuclear friction $\gamma_n = 0.003$. Note that the Marcus theory is valid in the small Γ regime, and the FEF method is valid in the large Γ regime.

is very small.⁴⁹ This is not true anymore when we have Floquet driving.

We now investigate the effects of the Floquet driving on the ET rate. In Figure 3, we plot the ET rate as a function of the driving frequency and driving amplitude. Here, we are in the strong nonadiabatic limit ($\Gamma = 0.0005$), such that we expect that the Floquet Marcus nonadiabatic theory works. Indeed, the Marcus rates agree with the results from FaSH-density (and FaSH) very well, both predicting that the ET rates increase rapidly with the driving amplitude A at the beginning and then gradually level off. There is no turnover of rates as a function of the driving amplitudes. For a donor–acceptor model with Floquet driving, one can show that there is a turnover of the rates as a function of the driving amplitudes.^{50,51} Such a turnover is similar to the trend from the Marcus normal region to the Marcus inverted region. With a continuum of acceptors from the metal surfaces, the Marcus inverted region does not exist, such that we do not see a turnover in the plot for the rates as a function of driving amplitude. That being said, we do see a turnover of the rates as a function of the driving frequency in Figure 3b. Clearly,

adding driving can increase the ET rates. However, when the driving is very fast, the electron does not see the driving, such that there are few effects on the ET rates.

To further verify the turnover effects, we plot the derivative of the Floquet Marcus rate on the driving amplitude and driving frequency in Figure 4. Also, see Appendix B in the Supporting Information. As we can see, $\frac{dk_{0 \rightarrow 1}}{dA}$ oscillates as a function of driving amplitude A and $\frac{dk_{0 \rightarrow 1}}{dA}$ is greater than 0 for all values of A , predicting that the ET rates always increase with A . In contrast, $\frac{dk_{0 \rightarrow 1}}{d\Omega}$ is greater than 0 for small Ω and smaller than 0 for larger Ω . The position where $\frac{dk_{0 \rightarrow 1}}{d\Omega} = 0$ gives rise to the turnover point.

In Figure 5, we further plot the ET rates as a function of driving amplitude and driving frequency in the weak nonadiabatic limit ($\Gamma = 0.005$). In such a regime, the Floquet Marcus theory fails, where the Floquet Marcus rates are much larger than the results obtained from FaSH-density and FaSH. Still, the dependence of the ET rates on driving amplitude and driving frequency is very similar to the case of small Γ . In particular, the optimal frequency Ω that predicts the maximal ET rates does not change with Γ .

The processes of ET rate calculation using Floquet surface hopping and Floquet electronic friction algorithms are given in Appendix C in Supporting Information.

CONCLUSIONS

In summary, we have formulated a Floquet Marcus theory to determine the ET rates at the molecule–metal interface under Floquet driving. Such a formula agrees with our Floquet surface hopping methods in the strong nonadiabatic limit. However, the Floquet Marcus theory fails in the weak nonadiabatic regime. In the weak nonadiabatic limit, the Floquet surface hopping approaches reproduce the Floquet electronic friction methods. In both cases, we found that ET rates increase monotonically with the driving amplitude. In contrast, the ET rates exhibit a turnover effect as a function of driving frequencies. Given the fact that ET rates at the molecule–metal interface can be significantly manipulated via Floquet engineering, we expect that our methods will be very

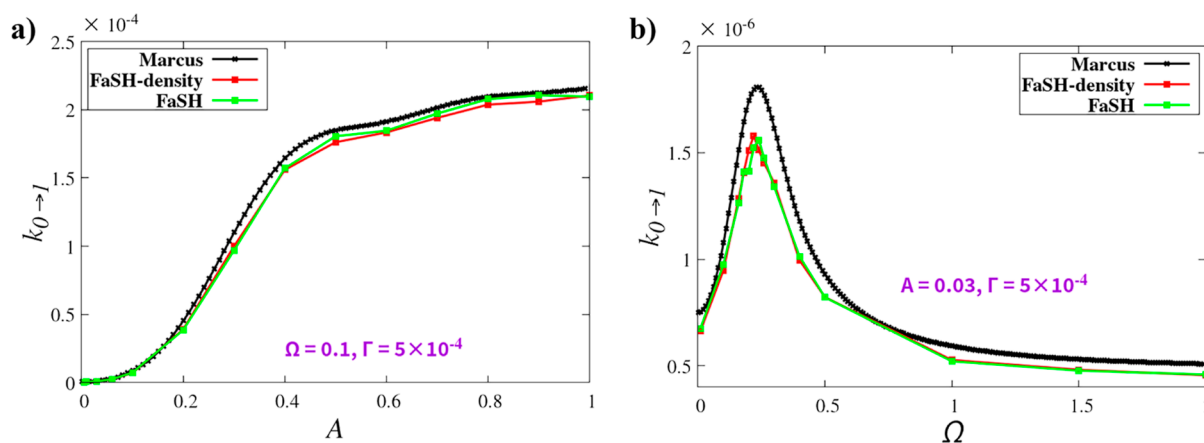


Figure 3. ET rates near the metal surface as a function of (a) driving amplitudes A ($\Omega = 0.1$) and (b) driving frequencies Ω ($A = 0.03$) at a small Γ limit ($\Gamma = 0.0005$). $kT = 0.01$, $\omega = 0.003$, $g = 0.025$, and $E_d = \frac{g^2}{\hbar\omega}$. Note that numerical surface hopping algorithms are consistent with Marcus rates in the small Γ limit. There is no turnover effect of ET rates as a function of A , while there is a turnover effect as a function of Ω .

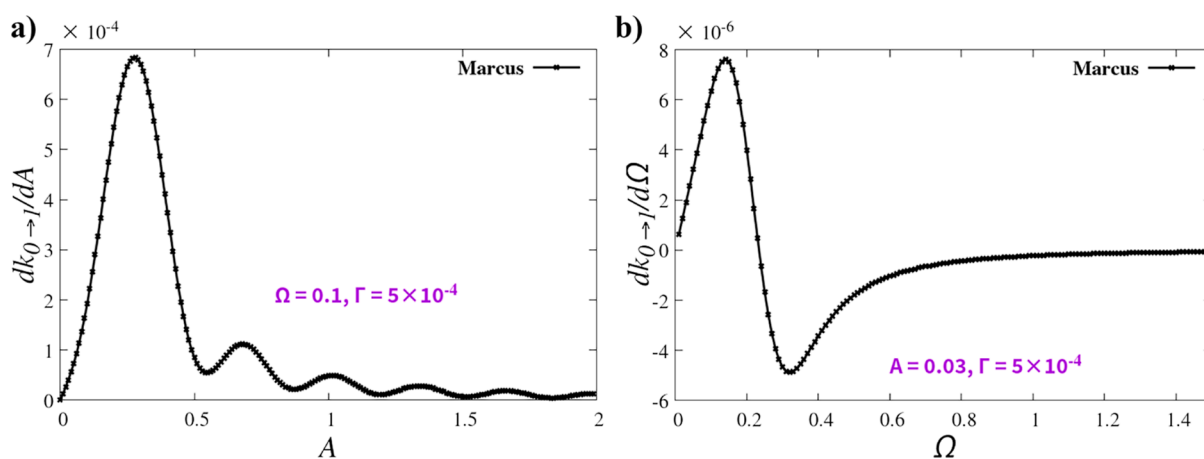


Figure 4. Analytical gradient of $k_{0 \rightarrow 1}$ with respect to (a) driving amplitude A and (b) driving frequency Ω . $kT = 0.01$, $\omega = 0.003$, $g = 0.025$, and $E_d = \frac{g^2}{\hbar\omega}$. Note that $dk_{0 \rightarrow 1}/dA \geq 0$, which means $k_{0 \rightarrow 1}$ increases with A until it reaches a plateau, while $dk_{0 \rightarrow 1}/d\Omega$ crosses over the zero point, thus demonstrating the turnover effect.

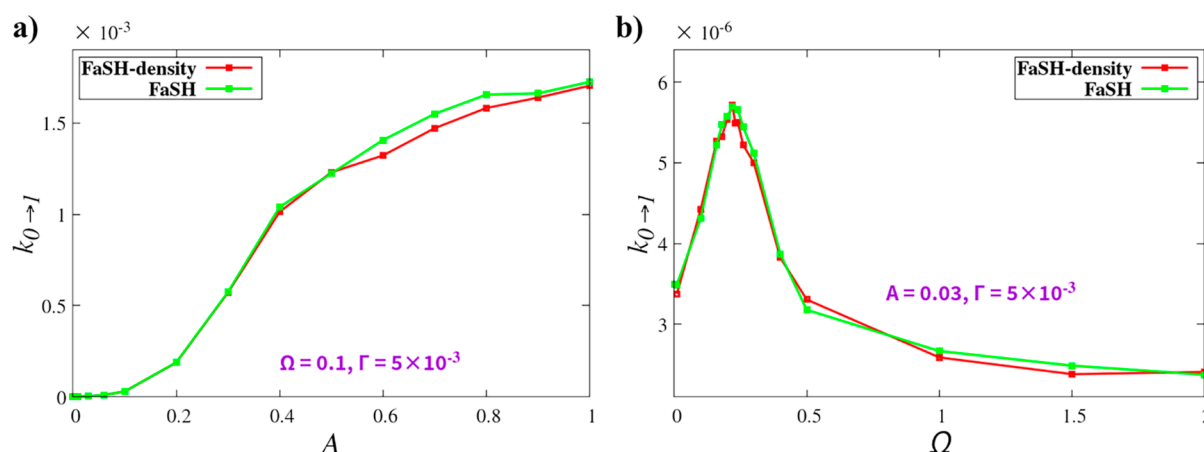


Figure 5. ET rates near the metal surface as a function of (a) driving amplitudes A ($\Omega = 0.1$) and (b) driving frequencies Ω ($A = 0.03$) at a large Γ limit ($\Gamma = 0.005$). $kT = 0.01$, $\omega = 0.003$, $g = 0.025$, and $E_d = \frac{g^2}{\hbar\omega}$. We see the same trends of ET rates as a function of A and Ω with those in Figure 3.

useful to study the nonadiabatic dynamics in photocatalysis, dye-sensitized solar cells, and chemisorptions.

■ ASSOCIATED CONTENT

Supporting Information

The Supporting Information is available free of charge at <https://pubs.acs.org/doi/10.1021/acsphyschemau.3c00049>.

Introduction of the Floquet electronic friction algorithm, derivatives of the Floquet Marcus rate, and calculation of ET rates with FSH and FEF methods step by step (PDF)

■ AUTHOR INFORMATION

Corresponding Author

Wenjie Dou – Department of Chemistry, School of Science, Westlake University, Hangzhou, Zhejiang 310024, China; Institute of Natural Sciences, Westlake Institute for Advanced Study, Hangzhou, Zhejiang 310024, China; orcid.org/0000-0001-5410-6183; Email: douwenjie@westlake.edu.cn

Author

Yu Wang – Department of Chemistry, School of Science, Westlake University, Hangzhou, Zhejiang 310024, China; Institute of Natural Sciences, Westlake Institute for Advanced Study, Hangzhou, Zhejiang 310024, China; orcid.org/0000-0001-7278-8608

Complete contact information is available at: <https://pubs.acs.org/10.1021/acsphyschemau.3c00049>

Notes

The authors declare no competing financial interest.

■ ACKNOWLEDGMENTS

This material is based upon the work supported by the National Natural Science Foundation of China (NSFC no. 22273075).

■ REFERENCES

(1) Lindstrom, C.; Zhu, X.-Y. Photoinduced electron transfer at molecule- metal interfaces. *Chem. Rev.* **2006**, *106*, 4281–4300.

- (2) Zhang, Y.; He, S.; Guo, W.; Hu, Y.; Huang, J.; Mulcahy, J. R.; Wei, W. D. Surface-plasmon-driven hot electron photochemistry. *Chem. Rev.* **2018**, *118*, 2927–2954.
- (3) Ge, A.; Rudshsteyn, B.; Zhu, J.; Maurer, R. J.; Batista, V. S.; Lian, T. Electron–hole-pair-induced vibrational energy relaxation of rhenium catalysts on gold surfaces. *J. Phys. Chem. Lett.* **2018**, *9*, 406–412.
- (4) Wang, Z.; Wang, X.; Wang, H.; Chen, X.; Dai, W.; Fu, X. The role of electron transfer behavior induced by CO chemisorption on visible-light-driven CO conversion over WO₃ and CuWO₄/WO₃. *Appl. Catal., B* **2020**, *265*, 118588.
- (5) Listorti, A.; O'regan, B.; Durrant, J. R. Electron transfer dynamics in dye-sensitized solar cells. *Chem. Mater.* **2011**, *23*, 3381–3399.
- (6) Wu, G.; Kong, F.; Li, J.; Chen, W.; Fang, X.; Zhang, C.; Chen, Q.; Zhang, X.; Dai, S. Influence of different acceptor groups in julolidine-based organic dye-sensitized solar cells. *Dyes Pigm.* **2013**, *99*, 653–660.
- (7) Zhang, X.; Wang, Y.; Liu, B.; Sang, Y.; Liu, H. Heterostructures construction on TiO₂ nanobelts: a powerful tool for building high-performance photocatalysts. *Appl. Catal., B* **2017**, *202*, 620–641.
- (8) Phuc, N. T.; Ishizaki, A. Control of quantum dynamics of electron transfer in molecular loop structures: Spontaneous breaking of chiral symmetry under strong decoherence. *Phys. Rev. B* **2019**, *99*, 064301.
- (9) Bukov, M.; D'Alessio, L.; Polkovnikov, A. Universal high-frequency behavior of periodically driven systems: from dynamical stabilization to Floquet engineering. *Adv. Phys.* **2015**, *64*, 139–226.
- (10) Oka, T.; Kitamura, S. Floquet engineering of quantum materials. *Annu. Rev. Condens. Matter Phys.* **2019**, *10*, 387–408.
- (11) Mandal, A.; Huo, P. Investigating new reactivities enabled by polariton photochemistry. *J. Phys. Chem. Lett.* **2019**, *10*, 5519–5529.
- (12) Cayssol, J.; Dóra, B.; Simon, F.; Moessner, R. Floquet topological insulators. *Phys. Status Solidi RRL* **2013**, *7*, 101–108.
- (13) Else, D. V.; Bauer, B.; Nayak, C. Floquet time crystals. *Phys. Rev. Lett.* **2016**, *117*, 090402.
- (14) Ghosh, A. K.; Nag, T.; Saha, A. Floquet generation of a second-order topological superconductor. *Phys. Rev. B* **2021**, *103*, 045424.
- (15) Herath, K.; Premaratne, M. Floquet engineering of dressed surface plasmon polariton modes in plasmonic waveguides. *Phys. Rev. B* **2022**, *106*, 235422.
- (16) Orgiu, E.; George, J.; Hutchison, J.; Devaux, E.; Dayen, J.; Doudin, B.; Stellacci, F.; Genet, C.; Schachenmayer, J.; Genes, C.; et al. Conductivity in organic semiconductors hybridized with the vacuum field. *Nat. Mater.* **2015**, *14*, 1123–1129.
- (17) Nagarajan, K.; George, J.; Thomas, A.; Devaux, E.; Chervy, T.; Azzini, S.; Joseph, K.; Jouaiti, A.; Hosseini, M. W.; Kumar, A.; et al. Conductivity and Photoconductivity of a p-Type Organic Semiconductor under Ultrastrong Coupling. *ACS Nano* **2020**, *14*, 10219–10225.
- (18) Zhong, X.; Chervy, T.; Zhang, L.; Thomas, A.; George, J.; Genet, C.; Hutchison, J. A.; Ebbesen, T. W. Energy transfer between spatially separated entangled molecules. *Angew. Chem.* **2017**, *129*, 9162–9166.
- (19) Dundas, D.; McCann, J. F.; Parker, J. S.; Taylor, K. T. Ionization dynamics of laser-driven H₂⁺. *J. Phys. B: At., Mol. Opt. Phys.* **2000**, *33*, 3261–3276.
- (20) Bukov, M.; Kolodrubetz, M.; Polkovnikov, A. Schrieffer-Wolff Transformation for Periodically Driven Systems: Strongly Correlated Systems with Artificial Gauge Fields. *Phys. Rev. Lett.* **2016**, *116*, 125301.
- (21) Bloch, J.; Caverlier, A.; Galitski, V.; Hafezi, M.; Rubio, A. Strongly correlated electron–photon systems. *Nature* **2022**, *606*, 41–48.
- (22) Babadi, M.; Knap, M.; Martin, I.; Refael, G.; Demler, E. Theory of parametrically amplified electron-phonon superconductivity. *Phys. Rev. B* **2017**, *96*, 014512.
- (23) Hübener, H.; De Giovannini, U.; Rubio, A. Phonon Driven Floquet Matter. *Nano Lett.* **2018**, *18*, 1535–1542.
- (24) Tikhonov, A.; Coalson, R. D.; Dahnovsky, Y. Calculating electron transport in a tight binding model of a field-driven molecular wire: Floquet theory approach. *J. Chem. Phys.* **2002**, *116*, 10909–10920.
- (25) Kohler, S.; Lehmann, J.; Hanggi, P. Driven quantum transport on the nanoscale. *Phys. Rep.* **2005**, *406*, 379–443.
- (26) Engelhardt, G.; Platero, G.; Cao, J. Discontinuities in driven spin-boson systems due to coherent destruction of tunneling: breakdown of the Floquet-Gibbs distribution. *Phys. Rev. Lett.* **2019**, *123*, 120602.
- (27) Cabra, G.; Franco, I.; Galperin, M. Optical properties of periodically driven open nonequilibrium quantum systems. *J. Chem. Phys.* **2020**, *152*, 094101.
- (28) Wu, B. H.; Cao, J. C. A Floquet–Green's function approach to mesoscopic transport under ac bias. *J. Phys.: Condens. Matter* **2008**, *20*, 085224.
- (29) Martinez, D. F. Floquet–Green function formalism for harmonically driven Hamiltonians. *J. Phys. A: Math. Gen.* **2003**, *36*, 9827–9842.
- (30) Chen, S.-H.; Chen, C.-L.; Chang, C.-R.; Mahfouzi, F. Spin-charge conversion in a multiterminal Aharonov-Casher ring coupled to precessing ferromagnets: A charge-conserving Floquet nonequilibrium Green function approach. *Phys. Rev. B: Condens. Matter Mater. Phys.* **2013**, *87*, 045402.
- (31) Qin, T.; Hofstetter, W. Spectral functions of a time-periodically driven Falicov-Kimball model: Real-space Floquet dynamical mean-field theory study. *Phys. Rev. B* **2017**, *96*, 075134.
- (32) Sandholzer, K.; Murakami, Y.; Görg, F.; Minguzzi, J.; Messer, M.; Desbuquois, R.; Eckstein, M.; Werner, P.; Esslinger, T. Quantum simulation meets nonequilibrium dynamical mean-field theory: Exploring the periodically driven, strongly correlated fermi-hubbard model. *Phys. Rev. Lett.* **2019**, *123*, 193602.
- (33) Moskalets, M.; Büttiker, M. Floquet scattering theory of quantum pumps. *Phys. Rev. B* **2002**, *66*, 205320.
- (34) Li, H.; Shapiro, B.; Kottos, T. Floquet scattering theory based on effective Hamiltonians of driven systems. *Phys. Rev. B* **2018**, *98*, 121101.
- (35) Moskalets, M. Floquet scattering matrix theory of heat fluctuations in dynamical quantum conductors. *Phys. Rev. Lett.* **2014**, *112*, 206801.
- (36) Zhou, Z.; Chen, H.-T.; Nitzan, A.; Subotnik, J. E. Nonadiabatic dynamics in a laser field: Using Floquet fewest switches surface hopping to calculate electronic populations for slow nuclear velocities. *J. Chem. Theory Comput.* **2020**, *16*, 821–834.
- (37) Schirò, M.; Eich, F. G.; Agostini, F. Quantum–classical nonadiabatic dynamics of Floquet driven systems. *J. Chem. Phys.* **2021**, *154*, 114101.
- (38) Wang, Y.; Dou, W. Nonadiabatic dynamics near metal surface with periodic drivings: A Floquet surface hopping algorithm. *J. Chem. Phys.* **2023**, *158*, 224109.
- (39) Wang, Y.; Dou, W. Nonadiabatic dynamics near metal surfaces under Floquet engineering: Floquet electronic friction vs Floquet surface hopping. *J. Chem. Phys.* **2023**, *159*, 094103.
- (40) Zhang, Z.; Zhang, C.; Zheng, H.; Xu, H. Plasmon-driven catalysis on molecules and nanomaterials. *Acc. Chem. Res.* **2019**, *52*, 2506–2515.
- (41) Chen, X.; Jensen, L. Morphology dependent near-field response in atomistic plasmonic nanocavities. *Nanoscale* **2018**, *10*, 11410–11417.
- (42) Landry, B. R.; Subotnik, J. E. Communication: Standard surface hopping predicts incorrect scaling for Marcus' golden-rule rate: The decoherence problem cannot be ignored. *J. Chem. Phys.* **2011**, *135*, 191101.
- (43) Mosallanejad, V.; Wang, Y.; Chen, J.; Dou, W. Floquet nonadiabatic dynamics in open quantum systems. **2023**, arXiv:2303.08501. arXiv preprint. . Submission Date: 2023-03-15.
- (44) Dou, W.; Nitzan, A.; Subotnik, J. E. Surface hopping with a manifold of electronic states. III. Transients, broadening, and the Marcus picture. *J. Chem. Phys.* **2015**, *142*, 234106.

(45) Zhou, G.; Zhang, M.; Chen, Z.; Zhang, J.; Zhan, L.; Li, S.; Zhu, L.; Wang, Z.; Zhu, X.; Chen, H.; et al. Marcus Hole Transfer Governs Charge Generation and Device Operation in Nonfullerene Organic Solar Cells. *ACS Energy Lett.* **2021**, *6*, 2971–2981.

(46) Anderson, N. A.; Lian, T. Ultrafast electron transfer at the molecule-semiconductor nanoparticle interface. *Annu. Rev. Phys. Chem.* **2005**, *56*, 491–519.

(47) Morton, S. M.; Jensen, L. Understanding the molecule- surface chemical coupling in SERS. *J. Am. Chem. Soc.* **2009**, *131*, 4090–4098.

(48) Dou, W.; Nitzan, A.; Subotnik, J. E. Frictional effects near a metal surface. *J. Chem. Phys.* **2015**, *143*, 054103.

(49) Ouyang, W.; Dou, W.; Jain, A.; Subotnik, J. E. Dynamics of Barrier Crossings for the Generalized Anderson–Holstein Model: Beyond Electronic Friction and Conventional Surface Hopping. *J. Chem. Theory Comput.* **2016**, *12*, 4178–4183.

(50) Su, Y.; Chen, Z.-H.; Zhu, H.; Wang, Y.; Han, L.; Xu, R.-X.; Yan, Y. Electron transfer under the Floquet modulation in donor–bridge–acceptor systems. *J. Phys. Chem. A* **2022**, *126*, 4554–4561.

(51) Thanh Phuc, N.; Ishizaki, A. Control of excitation energy transfer in condensed phase molecular systems by Floquet engineering. *J. Phys. Chem. Lett.* **2018**, *9*, 1243–1248.